scientific reports

Check for updates

OPEN

Formulation and characterization of nanofibrous scaffolds incorporating extracellular vesicles loaded with curcumin

Adrienn Kazsoki[1,6], Krisztina Németh[2,3,6], Tamás Visnovitz[2,4], Dorina Lenzinger[2], Edit I Buzás[2,3,5] & Romána Zelkó[1]✉

Due to their small size, flexibility, and adhesive properties, extracellular vesicles (EVs) hold promises as effective drug delivery systems. However, challenges such as the variability in vesicle types and the need to maintain their integrity for medical applications exist. Curcumin, a compound found in turmeric and known for its diverse health benefits, including anti-cancer and anti-inflammatory properties, faces obstacles in clinical use due to issues like low solubility, limited absorption, and rapid breakdown in the body. This study aimed to incorporate large-sized curcumin-loaded extracellular vesicles (lEVs) into fast-dissolving nanofibers made of poly(vinyl alcohol) (PVA) by electrospinning. By using aqueous PVA-based solutions for electrospinning, the presence of curcumin-loaded lEVs in the nanofibers was confirmed by confocal laser scanning microscopy. Furthermore, the release study demonstrated high concentrations of the drug in nanofibers containing lEVs. These findings are significant for advancing the development and utilization of active ingredient-loaded EV systems within nanofibrous formulations, potentially leading to improved patient outcomes.

Keywords Curcumin-loaded extracellular vesicle, Loading capacity, Nanofibrous formulation, Electrospinning, In vitro dissolution study

Abbreviations

EV	Extracellular vesicle
FBS	Fetal bovine serum
FI	Fluorescence intensity
IR	Ischemia–reperfusion
lEV	Large-sized extracellular vesicle
MESC-exocur	Curcumin loaded mouse embryonic stem cell exosome
NTA	Number of tracking analysis
PBS	Phoshate buffer saline
PVA	Poly(vinyl alcohol)
SEM	Standard error of the mean
sEV	Small-sized extracellular vesicle
SSC	Side scatter
TEM	Transmission electron microscopy

Over the past three decades, numerous studies have been published on the beneficial functional and biological properties of curcumin, such as its anti-inflammatory, antioxidant, antimutagenic, antimicrobial, antitumor, wound healing, and anti-angiogenesis effects[1–8]. Despite these advantages, the practical application of curcumin is limited by several factors, such as poor water solubility, physicochemical instability, low permeability, and

[1]University Pharmacy Department of Pharmacy Administration, Semmelweis University, Hőgyes Endre Street 7-9, Budapest 1092, Hungary. [2]Department of Genetics Cell and Immunobiology, Semmelweis University, Budapest, Hungary Nagyvárad Square 4, 1089 Budapest, Hungary. [3]HUN-REN Translational Extracellular Vesicle Research Group, Budapest, Hungary. [4]Department of Plant Physiology and Molecular Plant Biology, Faculty of Science, ELTE Eötvös Loránd University, 1117 Budapest, Hungary. [5]HCEMM-SU Extracellular Vesicle Research Group, Budapest, Hungary. [6]These authors contributed equally: Adrienn Kazsoki and Krisztina Németh. ✉email: zelko.romana@semmelweis.hu

low bioavailability due to poor absorption and rapid metabolism. Additionally, curcumin is sensitive to alkaline conditions, metal ions, heat, and light[9]. These obstacles, however, are being addressed by encapsulating curcumin in nano-formulations (nano-curcumin)[10]. Incorporation of curcumin into nanocarriers by various methods (liposomes, polymers, conjugates, cyclodextrins, micelles, dendrimers, and nanoparticles) is a suitable choice to enhance the bioactivity of curcumin, which increases its bioavailability and half-life[11–14], and reduce its potential undesirable effects on surrounding healthy cells/tissues.

Experimental data also support that the nano-formulation of curcumin is effective in treating liver and heart problems[15], cancers[16], and brain tumors[17].

Kalani et al. investigated whether a combined nano-formulation with curcumin-loaded mouse embryonic stem cell exosomes (MESC-exocur) restores neurovascular damage after ischemia-reperfusion (IR) injury in mice[18,19]. IR injury was induced in 8–10-week-old mice and they were divided into two groups. One of the two IR-injured groups received intranasally MESC-exocur for 7 days. The study found that MESC-exocur treatment reduced neurological score, infarct volume, and edema following IR injury. Compared with the untreated IR group, the MESC-exocur-treated IR group showed reduced inflammation and N-methyl-D-aspartate receptor expression. These results suggest that combining the potential of embryonic stem cell exosomes and curcumin may aid neurovascular recovery after ischemia-reperfusion injury in mice.

Nanofibers offer several unique advantages over other nanostructures for drug delivery applications[20]. Their high surface area-to-volume ratio allows for increased drug loading capacity and enhanced interaction with biological tissues. The porosity and interconnected structure of nanofibers mimic the extracellular matrix, providing an ideal scaffold for cell adhesion and proliferation while facilitating controlled drug release[21]. Furthermore, nanofibers offer versatility in material selection, allowing customization of mechanical properties and degradation rates using a wide range of biocompatible and biodegradable polymers[22]. Additionally, nanofibers are easily functionalized to improve drug loading, cellular interactions, and targeting capabilities, and they offer controlled and sustained release of encapsulated drugs over extended periods.

Nanofibers present additional benefits when combined with curcumin and extracellular vesicles (EVs). They protect curcumin from degradation, improving its stability -a key limitation of curcumin as a therapeutic agent -and enhance its bioavailability by increasing its dissolution rate[23]. Nanofibers also serve as an efficient co-delivery system for curcumin and EVs, potentially enhancing their synergistic effects. Nanofibers ensure more targeted treatment by enabling localized delivery to specific tissues or wound sites. Additionally, incorporating EVs into nanofibers may help preserve their integrity and biological activity while allowing for the controlled release of both curcumin and EVs, optimizing their therapeutic effects over time.

In this study, we aimed to combine the therapeutic potential of EVs with curcumin while preserving the stability of both the carrier vesicles and the encapsulated curcumin. To achieve these goals, we aimed to develop a curcumin-loaded EV-containing nanofibrous system through molecular packaging. Additionally, we sought to characterize the morphological behavior of these complex nanofibrous systems and evaluate their loading efficiency and drug release profiles, contributing to the advancement of hybrid drug delivery systems. By leveraging the unique advantages of nanofibers, this approach could help overcome the limitations of traditional delivery methods and enhance the therapeutic efficacy of curcumin and EVs as promising agents for various medical applications.

Materials and methods

Materials of the matrix of the drug delivery system

As the base of the formulation the biodegradable, biocompatible well, electrospinnable polymer poly(vinyl-alcohol) (PVA, Mowiol® 18–88, average molecular weight, M_w ~ 1,300,000 g/mol (Merck Ltd, Budapest, Hungary) was chosen. The sodium chloride (Molar Chemicals Ltd., Budapest, Hungary) was used to isotonization the precursor solution. As a solvent, distilled water of pharmaceutical grade without further purification was used.

Separation of lEVs

HEK293 cell line was maintained in DMEM cell culture medium (1 g/L glucose) supplemented with 10% Fetal Bovine Serum (FBS), streptomycin (1000 µg/L), penicillin (1000 U/L) and L-glutamine (2 mM) in a humidified atmosphere at 37 °C and 5% (V/V) CO_2. lEVs were separated from the conditioned medium of HEK293 cells. Cells were maintained in 8 flasks with a surface area of 182 cm^2 (VWR, USA) until cells reached 80–90% confluence, averaging 190×10^6 cells per separation. lEVs were separated 24 h after FBS deprivation using differential centrifugation. Briefly, conditioned cell medium was collected, and cells were removed by centrifugation (300 g, 10 min, 20 °C) and gravity filtration (pore size 5 µm, Sartorius, Germany). Subsequently, the extra-large-sized EVs (> 800–1000 nm, 2000 g, 30 min, 4 °C) and the lEVs (250–800 nm, 12,500 g, 40 min, 4 °C) were separated by increasing the centrifugal force. The lEV pellet was resuspended in phoshate buffer saline (PBS), then the sample was flash-frozen in liquid nitrogen and stored at -80 °C until use.

Curcumin loading of lEVs

Curcumin (Merck, Germany) was dissolved in absolute ethanol with mild rotation. The stock solution concentration was 1 mg/mL (2,700 µM), which was further diluted in PBS for labeling lEVs. Based on the preliminary experiments, lEVs were incubated with 150 µM curcumin for 30 min, at 37 °C, at neutral pH with shaking (Supplementary Fig. 1). The total amount (approximately ~ 8.2×10^8 particles) of lEVs obtained from the conditioned medium of cell culture per experiment was used for curcumin labeling in a final volume of 2 mL. The unbound curcumin molecules were removed by centrifugation (12,500 g, 40 min, 4 °C) and the lEV pellet was resuspended in 200 µL physiological saline solution. Buffer containing curcumin and lEV samples treated with ethanol were used as controls.

Parameter	lEV	Parameter	lEV
Sensitivity	60	Maximum brightness	20
Shutter	100	Minimum size (nm)	5
Frame rate	7.5	Maximum size (nm)	1000
Number of positions	11	Temperature (°C)	25
Number of cycles	2		

Table 1. Parameters of nanoparticle tracking analysis of large-size extracellular vesicles (lEV).

Sample	Flow rate (µL/sec)	Distance (cm)	Voltage (kV)	Emitter (G)
lEV + curcumin	0.08	12.5	25.1	22
sEV + curcumin	0.08	12.5	25.3	22

Table 2. Electrospinning process parameters of curcumin-loaded large-sized- and small-sized extracellular vesicles (lEVs and sEVs) containing precursor solutions. *collector-emitter distance.

Characterization of curcumin-loaded lEVs

Size distribution and particle number of lEVs

The particle number and median size of lEV samples were determined by Nanoparticle Tracking Analysis (NTA). Measurements were performed with a ZetaView PMX-120 (Particle Metrix GmbH, Meerbusch, Germany) using ZetaVIEW software according to the parameters summarized in Table 1.

Spectrophotometric analysis of lEVs

UV-visible absorption spectra of lEV samples were determined using a NanoDrop ND-1000 spectrophotometer (ThermoFisher, USA). The absorption maximum was measured at a wavelength of 420 nm.

Flow cytometric analysis of lEVs

Curcumin-loaded lEVs were characterized using CytoFLEX S (Beckman Coulter, USA) flow cytometer. The lEVs were diluted 300-fold in PBS and were characterized by Violet-SSC (Side SCatter) and by the intrinsic fluorescence of curcumin (excitation: 405 nm, detection: 610/20 nm). Events were detected for one minute at a medium flow rate (30 µL/min). The lEVs were measured using serial dilution to determine if single particles were being measured. HEK-293-derived lEVs were stained with Annexin V – A647 (1:800), α-human-CD81-PerCP/Cy5.5 (1:800), α-human-CD63-A647 (1:800), mouse-IgG1-PerCP/Cy5.5 (1:800) and mouse-IgG1-A647 (1:800). The presence of lEVs was validated by lysis with TritonX-100 (0.1%, Molar ChemicalsLtd., Hungary). All reagents used in these experiments are listed in Supplementary Table 1.

Characterization of lEVs by transmission electron miscroscopy (TEM)

TEM was used to examine the morphology of curcumin-loaded lEVs. Samples were prepared according to Théry et al. 2006 with minor modifications[24]. Briefly, approximately 2 µL of lEV sample was placed on the surface of a formvar-coated Ni grids (SPI Supplies, West Chester, PA, USA) and incubated for 10 min at room temperature. The remaining solution was removed and fixed with 2% glutaraldehyde for 10 min at room temperature. The grids were washed three times for 5 min by distilled water. The samples were contrasted and embedded in a mixture of UranyLess (#22409 EMS _ElectronMicroscopy Sciences, PA, USA) and 2% ultracentrifugated (100,000 g, 90 min, 4 °C) methylcellulose. Samples were examined by a JEOL 1011 transmission electron microscope. Olympus iTEM software (Japan) was used for images capturing, and for image analysis, Image J software was used.

Embedding curcumin-loaded lEVs into nanofibers

Preparation of precursor solution for electrospinning

For fiber formation, a 14% (w/v) aqueous solution of PVA was prepared and isotonized by the addition of NaCl. Separated lEVs were added to 1 g of viscous polymer solution in the separated volume (200 µL, $8{,}2 \times 10^8 \pm 3{,}9 \times 10^8$ particles/g PVA).

Electrospinning

The nanofibrous samples were prepared using a lab-scale electrospinning device from SpinSplit Ltd. The final process parameters were determined by monitoring the Taylor cone with the camera system of the device and scanning electron microscopy images.

The viscous polymer precursor solutions were loaded into a 1 mL plastic syringe (Merck Ltd., Budapest, Hungary) and connected to a 22G needle via a silicone tube. The syringe, once filled, was positioned on a pump to ensure a continuous flow of solution. Aluminum foil or baking paper was adhered to the collector to gather each sample for subsequent analysis. The procedure was conducted under ambient conditions, with a temperature of 22 ± 1 °C and relative humidity of 40 ± 5%. Table 2 summarizes the final process parameters used during fiber formation.

Characterization of curcumin-loaded lEV-containing PVA fibers by confocal laser scanning microscopy

PVA nanofibers filled with curcumin-loaded lEVs were examined using a Leica TCS SP8 confocal laser scanning microscope (Leica, Germany) with adaptive lightning using a HC PL APO CS2 63x/1.40 OIL immersion objective and hybrid detector. The resolution available with the microscope (d ~ 180 nm) allowed the examination of lEVs. PVA-lEV nanofibers were available on a 24 × 32 mm cover slide (VWR, USA). We identified HEK293-derived curcumin^{+} lEVs with 405 nm excitation and broad-range detection (approximately 410 nm to 565 nm). The PVA nanofibers were detected by transmitted light. For image analysis, Leica LASX software was used.

Characterization of drug release from a nanofibrous system

The dissolution test was carried out in 10 mL of isotonic water. Approximately 30 mg of fibrous sample was weighed and coiled on a 1 cm long magnetic stirring bead and placed in a 4 mm diameter steel spiral, ensuring that the nanofibers were not floating on the surface of the dissolution medium but were fully immersed in it. The release of the drug was monitored for 30 min using an in-line probe Jasco-V-750 UV-VIS spectrophotometer (ABL&E-JASCO Magyarország Ltd., Budapest, Hungary) at 420 nm. The drug concentration was determined after preliminary calibration and partial analytical method validation.

Statistical analysis

Values are shown as mean ± standard error of the mean (SEM). The statistical analysis was prepared using GraphPad Prism 7.00 (USA) software. Two-way ANOVA and Tukey's posthoc tests were used to compare the data. A *p*-value of less than 0.05 was accepted as statistically significant.

Results and discussion

Characterization of curcumin-loaded lEVs

Based on the NTA measurements, the median size of the curcumin-loaded lEVs was 333.6 ± 3.2 nm (span: 177,2 ± 14.3 nm), with $8.2 \times 10^8 \pm 3.9 \times 10^8$ particle number per separation (Fig. 1A). The span value was calculated as (D90 - D10) / D50, where D90, D10, and D50 are the particle diameters at 90%, 10%, and 50% of the cumulative distribution, respectively. A smaller span indicates a narrower size distribution.

Curcumin of the same concentration dissolved in buffer did not form detectable amounts of particles. In TEM photographs, curcumin-loaded lEVs showed a typical EV morphology (Fig. 1B). The result of the determination of 100 vesicles, 117.3 ± 40.7 nm average size was achieved. Based on the serial dilution, the number of events showed a linear correlation with the dilution factor, and the median fluorescence intensity of curcumin remained constant, so we can conclude that the measurements were performed at optimal dilution and were able to detect singlet particles (Supplementary Fig. 2). Buffer and unlabeled lEVs did not, but curcumin dissolved in buffer showed a slight fluorescence intensity. Compared to control samples, curcumin-labelled lEVs showed significantly higher fluorescence intensity. Curcumin positive events were lysable with TritonX-100 solution (0.1%(V/V)) (Fig. 1C). lEVs were characterized based on EV markers[25]. HEK293-derived lEVs were AnnexinV and CD63 positive and CD81 negative (Fig. 1D). Based on our UV-VIS spectrophotometric measurements, the curcumin-loaded lEVs showed significantly higher absorbance values (Fig. 1E).

Characterization of curcumin-loaded lEV-based PVA nanofibers by confocal laser scanning microscopy

EVs were successfully detected in curcumin-labeled HEK293-derived lEV-containing PVA nanofibers based on the fluorescence of curcumin (Fig. 2).

This figure shows confocal microscopy images of PVA nanofibers containing curcumin-loaded lEVs. The green fluorescence represents curcumin-loaded lEVs, while the PVA nanofibers are visualized using transmitted light. The images demonstrate the successful incorporation of curcumin-loaded lEVs within the PVA nanofiber matrix. The discrete green, fluorescent spots indicate individual or small clusters of curcumin-loaded lEVs distributed throughout the nanofiber structure. This visualization confirms the presence and distribution of drug-loaded vesicles within the electrospun fibers, validating the effectiveness of the encapsulation process and providing insight into the spatial arrangement of the therapeutic cargo within the scaffold.

Curcumin release from nanofibrous scaffolds

The drug release profiles of various fibrous samples are depicted in Fig. 3.

The dissolution profile of curcumin-loaded vesicle-containing PVA-based nanofibers can be influenced by several factors related to the properties of both the curcumin and the nanofibers, e.g., the drug's encapsulation efficiency, nanofiber morphology, PVA concentration, vesicle stability, and the conditions of the dissolution medium. It's important to note that during the experiments, the PVA concentration in the precursor solutions remained the same, and within the fiber diameter, no remarkable difference was obtained. The same dissolution medium and conditions were meticulously applied during the dissolution test.

The radii of vesicles within curcumin-loaded vesicle-containing PVA nanofibers significantly influence the release profile of curcumin. It investigated how vesicle size affects the release characteristics[26,27]. The main factors the surface area to volume ratio, diffusion path length, and the encapsulation efficiency were investigated.

The surface area to volume ratio plays a crucial role in the release of curcumin from vesicles. Smaller vesicles, with their higher surface area to volume ratio, provide a larger area for curcumin to contact the dissolution medium. This facilitates a faster initial release of curcumin, as more encapsulated curcumin is closer to the surface and can diffuse out more readily .The diffusion path length is a critical factor in the release of curcumin from vesicles. In smaller vesicles, the path for curcumin to travel from the center of the vesicle to the exterior is shorter. This shorter path allows for a quicker release of curcumin. In contrast, larger vesicles have a longer

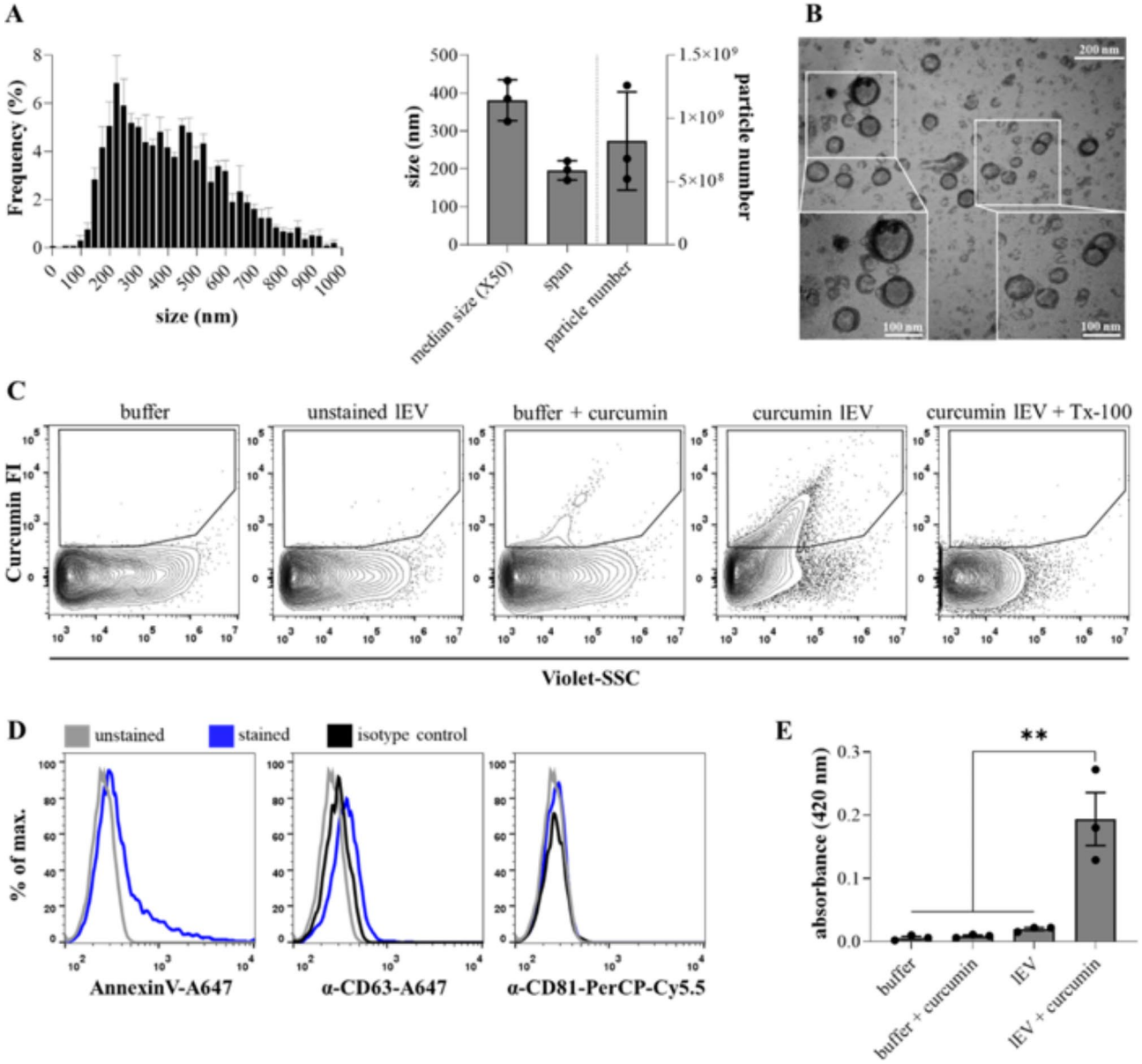

Fig. 1. Characterization of curcumin-loaded lEVs. The size distribution and particle concentration of curcumin-loaded lEVs was analyzed by nanoparticle tracking analysis (NTA) (**A**) and their morphology by transmission electron microscopy (TEM) (**B**). To investigate the association of curcumin with vesicles, curcumin-loaded lEVs were detected by flow cytometry-based on the intrinsic fluorescence of curcumin (**C**). Furthermore, the presence of lEVs was determined by analysis of EV marker (phosphatidylserine, CD63, CD81) expression (**D**). The absorbance (at 420 nm) of curcumin-labelled lEVs was also determined by UV-VIS spectrophotometry (E). Values are reported as mean ± SEM p value is calculated by ordinary one-way ANOVA with Tukey multiple comparisons test. $^{**}p < 0.01$, FI: fluorescence intensity, SSC: side scatter, lEV: large-sized extracellular vesicle.

diffusion path, potentially resulting in a slower and more sustained release of curcumin.The size of the vesicles can impact the encapsulation efficiency of curcumin.

To demonstrate how the vesicle size affects the cumin-loading efficacy of different vesicle sizes, we used a curcumin solution with an initial concentration of 150 μM. The loading was based on passive diffusion, considering the permeability of curcumin. These specific experimental conditions and methods were chosen to provide a clear understanding of the research process and its implications.

The following assumptions are made: the vesicles are spherical (1), the curcumin.

is uniformly distributed within the vesicle (2), the loading efficiency decreases with specific surface area (3) and the permeability of curcumin affects the diffusion rate across the vesicle membrane.

Vesicle Geometry can be described with the following equitations:

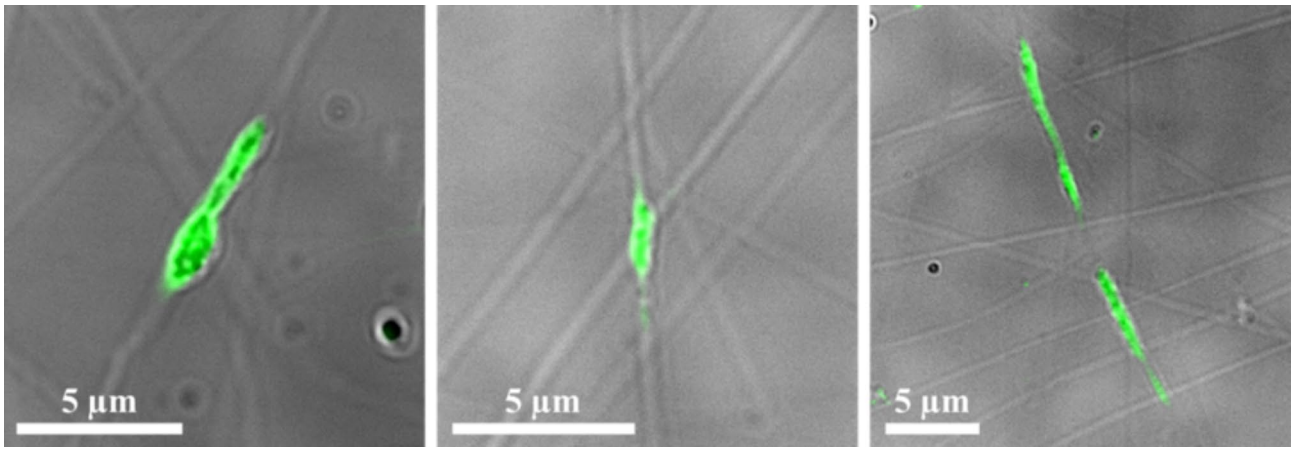

Fig. 2. Detection of curcumin-loaded lEVs in poly(vinyl alcohol) (PVA) nanofibers using confocal laser scanning microscopy, where the green fluorescence represents curcumin-loaded lEVs, while the PVA nanofibers are visualized using transmitted light.

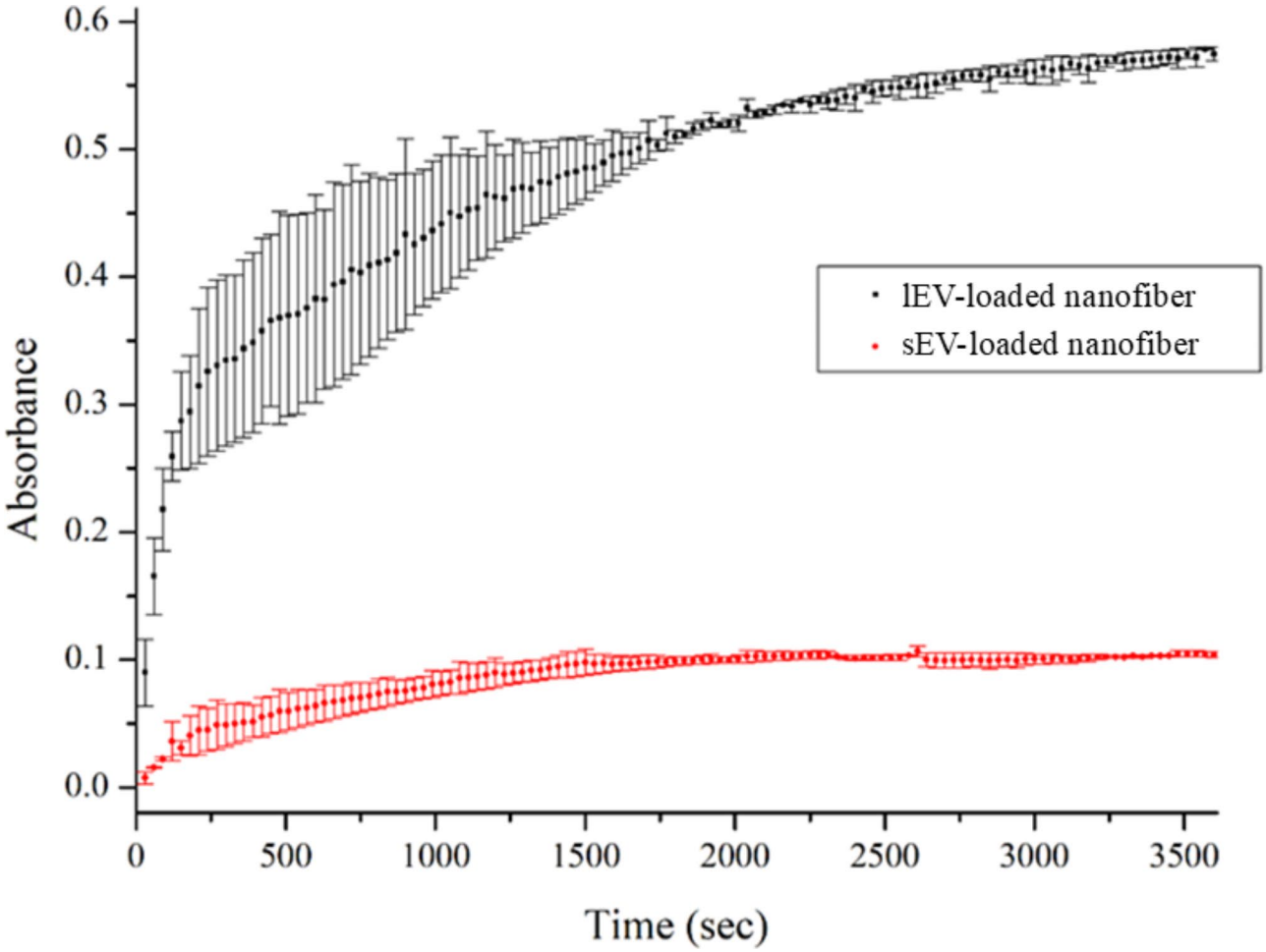

Fig. 3. Dissolution curves of nanofibrous samples containing curcumin-loaded small or large extracellular vesicles (sEV-loaded nanofiber or lEV-loaded nanofiber).

$$\text{Surface area: } A = 4\pi r^2 \tag{1}$$

$$\text{Volume: } V = \frac{4}{3}\pi r^3 \tag{2}$$

$$\text{Specific surface area: } \frac{A}{V} = \frac{4\pi r^2}{\frac{4}{3}\pi r^3} = \frac{3}{r} \tag{3}$$

where r is the radius of the spherical vesicle.

Loading efficiency (E) is assumed to decrease with increasing specific surface area, modeled as:

$$E = k\left(\frac{r}{3}\right)^n \tag{4}$$

where (k) and (n) are constants.

Permeability was also taken into account, because the permeability (P) of curcumin affects the rate at which it diffuses across the vesicle membrane. The flux (J) (amount of curcumin per unit time per unit area) is given by:

$$J = P \cdot (C_0 - C_{inside}) \tag{5}$$

where (C_{inside}) is the concentration of curcumin inside the vesicle.

Total curcumin flux into the vesicle is:

$$\text{Total Flux} = J \cdot A = P \cdot (C_0 - C_{inside}) \cdot 4\pi r^2 \tag{6}$$

At steady state, the rate of curcumin entering the vesicle equals the rate at which it distributes inside, leading to the steady-state concentration (C_{inside}).

The total amount of curcumin loaded in a vesicle can be approximated by considering the permeability effect on loading efficiency:

$$\text{Curcumin Loaded} = E * V * C_0 = k\left(\frac{r}{3}\right)^n \times \frac{4}{3}\pi r^3 \times C_0 \tag{7}$$

Python code was created for the model implementation, and plots were generated to show the relationship between vesicle radius, loading efficiency, and total curcumin loaded (Fig. 4).

Figure 4 illustrates the relationship between extracellular vesicle (EV) size and curcumin loading characteristics. The graph consists of two y-axes: the left y-axis (blue) represents the curcumin loading efficiency (%) into EVs. In contrast, the right y-axis (red) shows the total amount of curcumin loaded. The x-axis represents the radius of the extracellular vesicles in micrometers.

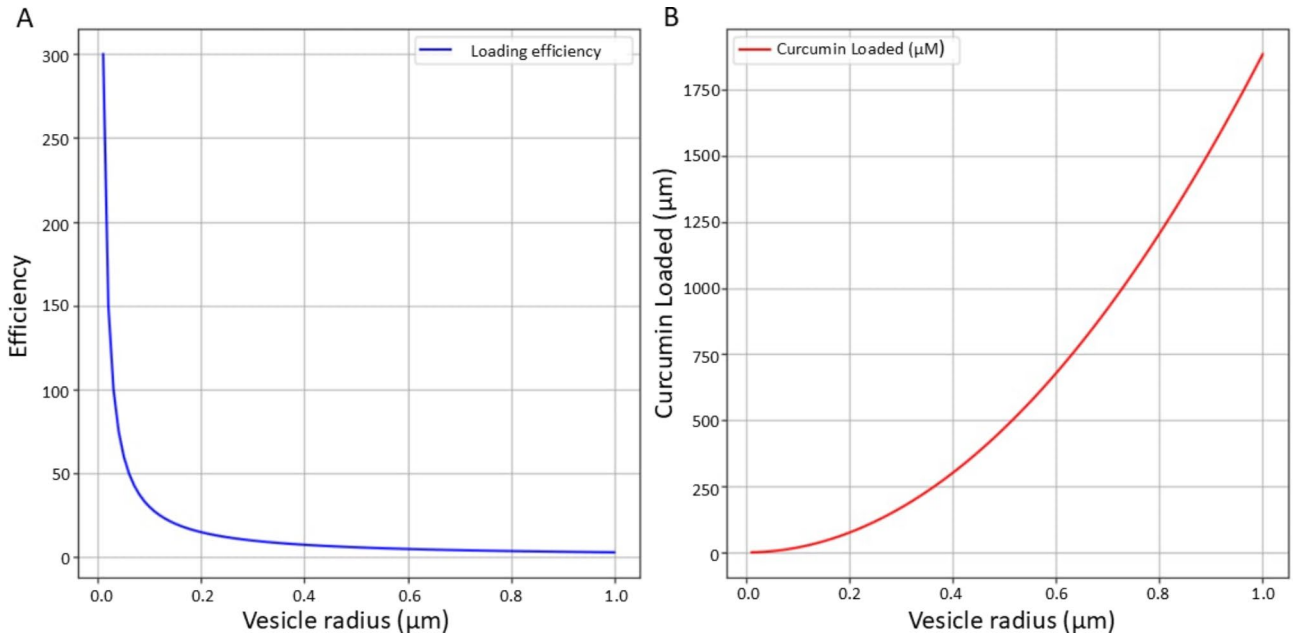

Fig. 4. Effect of the radii of the extracellular vesicle on the loading efficiency(A) and on the curcumin-loaded (B).

The blue curve demonstrates how loading efficiency changes with vesicle size. It shows a decrease in efficiency as vesicle radius increases, likely due to larger vesicles' decreasing surface area-to-volume ratio.

The orange curve illustrates the total amount of curcumin loaded into vesicles of different sizes. This curve shows an initial increase with vesicle size, reaching a maximum, then decreasing for very large vesicles.

This figure highlights the complex relationship between vesicle size, loading efficiency, and total drug loading capacity. It suggests an optimal vesicle size range for maximizing curcumin encapsulation, which is crucial for designing effective drug delivery systems using extracellular vesicles. Considering the above, the following can be said about the kinetics: due to the longer diffusion path and potentially slower degradation rate, larger vesicles might provide a more controlled and sustained release of curcumin.

The Weibull distribution was used to study the release kinetics of the different-size extracellular vesicle-loaded samples[28].

$$y = a - (a - b) * \exp\left(-(k * x)^{d}\right) \tag{8}$$

where y is the independent variable (absorbance), x is the dependent variable (time), a is the upper bound of y, while b is the lower bound of y, k is the scale parameter, and d is the shape parameter. The release parameters are summarized in Table 3.

The results showed that in the case of the sEV-loaded nanofiber system, the shape parameter was approximately 1, indicating the distribution simplifies to an exponential distribution. The shape parameter of the lEV-loaded nanofibrous sample was < 0.75, indicating Fickian diffusion[29].

For the larger EVs (lEV fiber), the release profile shows a rapid initial burst release phase, during which the curcumin concentration increases sharply, reaching saturation in approximately 250 s. This initial burst release can be attributed to the rapid diffusion of curcumin molecules from the surface and near-surface regions of the nanofibers. After this initial burst, the release rate slows and follows a more gradual, zero-order kinetic profile. This second phase likely represents the sustained release of curcumin encapsulated within the EVs or trapped within the nanofiber matrix, governed by diffusion and erosion mechanisms. After the saturation point, the release profile transitions to a zero-order kinetic phase, like the larger EVs, representing the sustained release of encapsulated or trapped curcumin.

The biphasic nature of the release profiles can be attributed to the interplay between the rapid release of surface-associated curcumin and the slower, diffusion-controlled release of encapsulated or trapped curcumin within the EVs and nanofiber matrix[30].

For further interpretation, a combined biphasic model was used:

$$C(t) = C_0\left(1 - e^{-k_1 t}\right) + k_2 t \tag{9}$$

where $_0$ is the initial concentration of curcumin available for burst release, $_1$ is the First-order rate constant for the initial burst release, and $_2$ is the zero-order rate constant for the sustained release. The fitted curve can be seen in Fig. 5. The optimized parameters were the following: $c_0 = 0.3774$, $k_1 = 0.0072$, $k_2 = 6.3228\text{e-}05$.

The primary mechanism of curcumin release can vary with vesicle size. The release might be dominated by diffusion through the PVA matrix and the vesicle membrane for smaller vesicles. For larger vesicles, the release might be controlled by the degradation of the vesicle and the PVA matrix.

To summarize, the size of the vesicles within curcumin-loaded vesicle-containing PVA nanofibers plays a crucial role in determining the release profile. Smaller vesicles tend to release curcumin quickly due to a higher surface area-to-volume ratio and shorter diffusion paths, while larger vesicles can provide a more controlled and sustained release.

The relationship between the dissolution profile of curcumin-loaded vesicle-containing PVA nanofibers and a combination of factors, including encapsulation efficiency, nanofiber morphology, PVA concentration, vesicle stability, and the conditions of the dissolution medium, is complex and influenced by a combination of factors.

Sample: sEV-loaded nanofiber				
Model	**SWeibull2**		**Value**	**Standard error**
Equitation	y = a - (a-b)*exp(-(k*x)^d)	a	0.10412	6.45E-04
Reduced Chi-Sqr	7.38E-06	b	0.0128	0.0024
Adj. R-Square	0.98454	d	0.98869	0.04872
		k	0.00147	4.93E-05
Sample: lEV-loaded nanofiber				
Model	**SWeibull2**		**Value**	**Standard error**
Equitation	y = a - (a-b)*exp(-(k*x)^d)	a	0.74279	5.84E-02
Reduced Chi-Sqr	9.03E-05	b	0	0.04736
Adj. R-Square	0.98996	d	0.3986	0.0591
		k	7.93E-04	1.74E-04

Table 3. Weibull-fitting parameters of curcumin-containing small- or large-sized extracellular vesicles (sEV or lEV)-loaded nanofibrous samples.

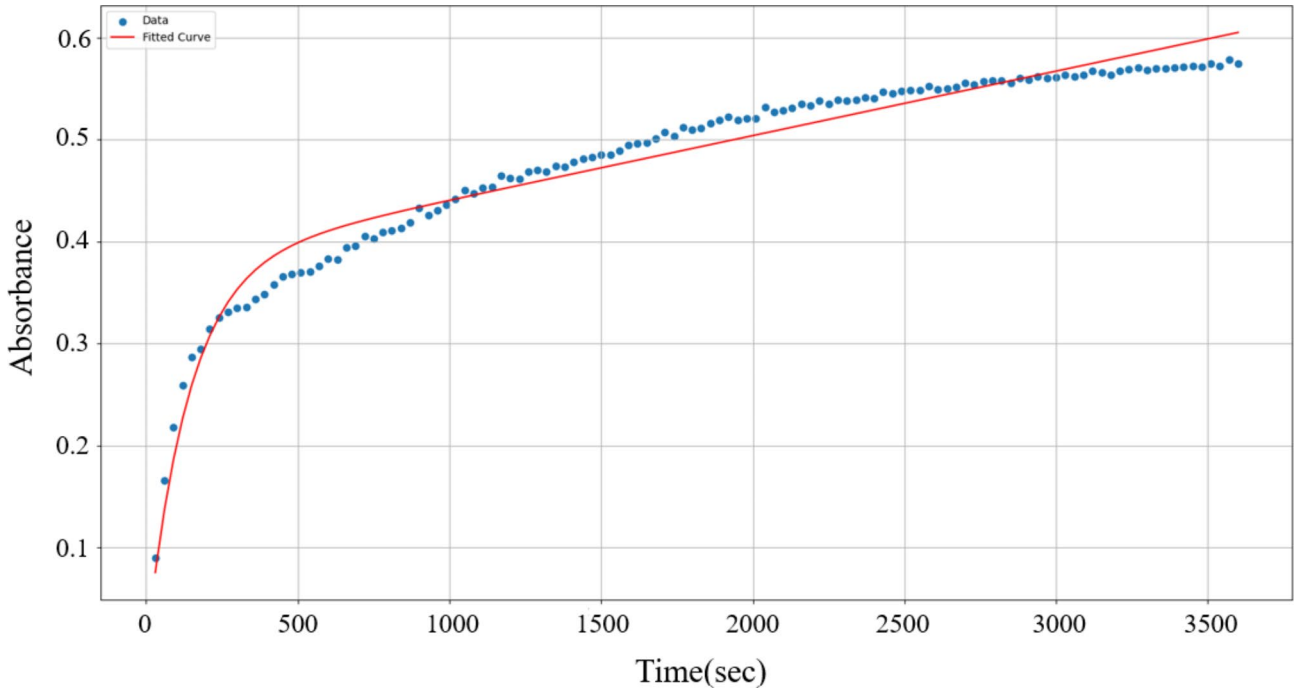

Fig. 5. Biphase curve fit of the lEV-loaded nanofibrous sample.

Optimizing these factors can lead to tailored release profiles suitable for various biomedical applications. The optimal vesicle size depends on the specific application and desired release kinetics for curcumin[31].

Conclusions

Based on the findings, it has been successfully demonstrated that curcumin can effectively optimize the loading of medium and small extracellular vesicles derived from HEK293 cells. Specifically, curcumin at a concentration of 150 μM, incubated at 37 °C with a near-neutral pH for 30 min, serves as an efficient loading agent for these extracellular vesicles. The presence of curcumin-loaded particles was confirmed through both spectrophotometry and flow cytometry.

Additionally, nanofibrous scaffolds were successfully created from precursor solutions containing various vesicles. Confocal microscopy allowed for the detection of curcumin-loaded large vesicles within polyvinyl alcohol (PVA) nanofibers. A release study indicated that higher drug concentrations were found in nanofibers containing larger vesicles. Notably, curcumin was released from the fiber samples relatively quickly, regardless of the size of the embedded vesicles.

This research underscores the innovative potential of integrating extracellular vesicles (EVs) with nanofibrous scaffolds to develop advanced drug delivery systems. The combination introduced several scientific advancements: it merges biological and synthetic components, combining the therapeutic benefits of EVs with the structural advantages of nanofibers to form a hybrid drug delivery system. This synergistic approach enhances drug delivery capabilities, offering superior control over drug release kinetics compared to using either component alone. Furthermore, the nanofiber matrix helps maintain the structural integrity of EVs, which is crucial for preserving their therapeutic efficacy. Additionally, this innovative strategy allows for tailored release profiles by adjusting the EV size and the properties of the nanofibers, enabling the fine-tuning of drug release for specific therapeutic applications. Furthermore, the encapsulation of EVs within the nanofibers improves the overall stability of the drug-loaded EVs, potentially extending their shelf life and efficacy.

Despite these promising results, several limitations require further consideration. These include challenges in the dosing as the vesicle loading and the drug content can be limited, controlled drug release, manufacturing complexity, potential bioactivity loss during electrospinning, immune response variability, and difficulties in scaling production for clinical use. Addressing these challenges will be crucial for translating this technology from research to therapeutic applications.

Despite all this, combining curcumin-loaded EVs within PVA nanofibers introduces an advanced strategy for drug delivery with customizable release profiles. This method enables fine-tuning of drug release based on EV size and nanofiber properties, enhancing stability and potentially extending shelf life and efficacy. By encapsulating EVs in nanofibers, this approach offers significant advancements in targeted delivery, improving bioavailability and therapeutic potential for agents like curcumin.

Data availability

All data generated or analyzed during this study are included in this published article and its supplementary information files.

Received: 13 June 2024; Accepted: 7 November 2024
Published online: 11 November 2024

References

1. Mahady, G. B., Pendland, S. L., Yun, G. & Lu, Z. Z. Turmeric (Curcuma longa) and curcumin inhibit the growth of Helicobacter pylori, a group 1 carcinogen. *Anticancer Res.* **22**, 4179–4181 (2002).
2. Aggarwal, B. B. & Harikumar, K. B. Potential therapeutic effects of curcumin, the anti-inflammatory agent, against neurodegenerative, cardiovascular, pulmonary, metabolic, autoimmune and neoplastic diseases. *Int. J. Biochem. Cell Biol.* **41**, 40–59. https://doi.org/10.1016/j.biocel.2008.06.010 (2009).
3. Akbik, D., Ghadiri, M., Chrzanowski, W. & Rohanizadeh, R. Curcumin as a wound healing agent. *Life Sci.* **116**, 1–7. https://doi.org/10.1016/j.lfs.2014.08.016 (2014).
4. Hu, K. et al. Core–shell biopolymer nanoparticle delivery systems: synthesis and characterization of curcumin fortified zein–pectin nanoparticles. *Food Chem.* **182**, 275–281. https://doi.org/10.1016/j.foodchem.2015.03.009 (2015).
5. Silva, A. C. et al. Impact of curcumin nanoformulation on its antimicrobial activity. *Trends Food Sci. Technol.* **72**, 74–82. https://doi.org/10.1016/j.tifs.2017.12.004 (2018).
6. Imran, M. et al. Cucurmin, anticancer, & antitumor perspectives: a comprehensive review. *Crit. Rev. Food Sci. Nutr.* **58**, 1271–1293. https://doi.org/10.1080/10408398.2016.1252711 (2018).
7. Willenbacher, E. et al. Curcumin: new insights into an ancient ingredient against cancer. *Int. J. Mol. Sci.* **20** (2019).
8. Fernández-Bedmar, Z. & Alonso-Moraga, A. Vivo and in vitro evaluation for nutraceutical purposes of capsaicin, capsanthin, lutein and four pepper varieties. *Food Chem. Toxicol.* **98**, 89–99. https://doi.org/10.1016/j.fct.2016.10.011 (2016).
9. Flora, G., Gupta, D. & Tiwari, A. Preventive efficacy of bulk and nanocurcumin against lead-Induced oxidative stress in mice. *Biol. Trace Elem. Res.* **152**, 31–40. https://doi.org/10.1007/s12011-012-9586-3 (2013).
10. Yallapu, M. M., Jaggi, M. & Chauhan, S. C. Curcumin nanoformulations: a future nanomedicine for cancer. *Drug Discovery Today*. **17**, 71–80. https://doi.org/10.1016/j.drudis.2011.09.009 (2012).
11. Sahu, A., Kasoju, N. & Bora, U. Fluorescence study of the curcumin – casein Micelle complexation and its application as a drug nanocarrier to cancer cells. *Biomacromolecules*. **9**, 2905–2912. https://doi.org/10.1021/bm800683f (2008).
12. Das, R. K., Kasoju, N. & Bora, U. Encapsulation of curcumin in alginate-chitosan-pluronic composite nanoparticles for delivery to cancer cells. *Nanomed. Nanotechnol. Biol. Med.* **6**, 153–160. https://doi.org/10.1016/j.nano.2009.05.009 (2010).
13. Li, G., Xu, L., Jiang, M. & Wu, X. Eye drops and eye gels of levofloxacin: comparison of ocular absorption characterizations and therapeutic effects in the treatment of bacterial keratitis in rabbits. *Drug Dev. Ind. Pharm.* **46**, 673–681. https://doi.org/10.1080/03639045.2020.1750626 (2020).
14. Fonseca-Santos, B., dos Santos, A. M., Rodero, C. F., Gremião, M. P. D. & Chorilli, M. Design, characterization, and biological evaluation of curcumin-loaded surfactant-based systems for topical drug delivery. *Int. J. Nanomed.* **11**, 4553–4562. https://doi.org/10.2147/IJN.S108675 (2016).
15. Shimatsu, A. et al. Clinical application of curcumin, a multi-functional substance.
16. Mohanty, C. & Sahoo, S. K. The in vitro stability and in vivo pharmacokinetics of curcumin prepared as an aqueous nanoparticulate formulation. *Biomaterials*. **31**, 6597–6611. https://doi.org/10.1016/j.biomaterials.2010.04.062 (2010).
17. Lim, K. J., Bisht, S., Bar, E. E., Maitra, A. & Eberhart, C. G. A polymeric nanoparticle formulation of curcumin inhibits growth, clonogenicity and stem-like fraction in malignant brain tumors. *Cancer Biol. Ther.* **11**, 464–473. https://doi.org/10.4161/cbt.11.5.14410 (2011).
18. Kalani, A. et al. Curcumin-loaded embryonic stem cell exosomes restored neurovascular unit following ischemia-reperfusion injury. *Int. J. Biochem. Cell Biol.* **79**, 360–369. https://doi.org/10.1016/j.biocel.2016.09.002 (2016).
19. Kalani, A. & Chaturvedi, P. Curcumin-primed and curcumin-loaded exosomes: potential neural therapy. *Neural Regen Res.* **12**, 205–206. https://doi.org/10.4103/1673-5374.200799 (2017).
20. Leung, V. & Ko, F. Biomedical applications of nanofibers. *Polym. Adv. Technol.* **22**, 350–365. https://doi.org/10.1002/pat.1813 (2011). https://doi.org/https://doi.org/
21. Garkal, A., Kulkarni, D., Musale, S., Mehta, T. & Giram, P. Electrospinning nanofiber technology: a multifaceted paradigm in biomedical applications. *New J. Chem.* **45**, 21508–21533. https://doi.org/10.1039/D1NJ04159B (2021).
22. Jayaraman, K., Kotaki, M., Zhang, Y., Mo, X. & Ramakrishna, S. Recent advances in polymer nanofibers. *J. Nanosci. Nanotechnol.* **4**, 52–65. https://doi.org/10.1166/jnn.2004.078 (2004).
23. Németh, K. et al. Nanofiber formation as a promising technology for preservation and easy storage of extracellular vesicles. *SCI. REP.* **12**, 22012. https://doi.org/10.1038/s41598-022-25916-6 (2022).
24. Théry, C., Amigorena, S., Raposo, G. & Clayton, A. Isolation and characterization of exosomes from cell culture supernatants and biological fluids. *Curr. Protocols Cell. Biology*. **30**, 3.22.21–23.22.29 https://doi.org/10.1002/0471143030.cb0322s30 (2006).
25. Welsh, J. A. et al. Minimal information for studies of extracellular vesicles (MISEV2023): from basic to advanced approaches. *Journal of Extracellular Vesicles* **13**, e12404 https://doi.org/10.1002/jev2.12404 (2024).
26. Pattni, B. S., Chupin, V. V. & Torchilin, V. P. New developments in liposomal drug delivery. *Chem. Rev.* **115**, 10938–10966. https://doi.org/10.1021/acs.chemrev.5b00046 (2015).
27. Siepmann, J. & Siepmann, F. Modeling of diffusion controlled drug delivery. *J. Controlled Release*. **161**, 351–362. https://doi.org/10.1016/j.jconrel.2011.10.006 (2012).
28. Papadopoulou, V., Kosmidis, K., Vlachou, M. & Macheras, P. On the use of the Weibull function for the discernment of drug release mechanisms. *Int. J. Pharm.* **309**, 44–50. https://doi.org/10.1016/j.ijpharm.2005.10.044 (2006).
29. Ritger, P. L. & Peppas, N. A. A simple equation for description of solute release I. Fickian and non-fickian release from non-swellable devices in the form of slabs, spheres, cylinders or discs. *J. Controlled Release*. **5**, 23–36. https://doi.org/10.1016/0168-3659(87)90034-4 (1987).
30. Siepmann, J. & Siepmann, F. Mathematical modeling of drug delivery. *Int. J. Pharm.* **364**, 328–343. https://doi.org/10.1016/j.ijpharm.2008.09.004 (2008).
31. Zylberberg, C. & Matosevic, S. Pharmaceutical liposomal drug delivery: a review of new delivery systems and a look at the regulatory landscape. *Drug Deliv.* **23**, 3319–3329. https://doi.org/10.1080/10717544.2016.1177136 (2016).

Acknowledgements

Adrienn Kazsoki thanks Gergő Nochta for his help with the Python code. The authors are also grateful to Houssam Abboud (University Pharmacy Department of Pharmacy Administration, Semmelweis University) for his help with the dissolution study.

Author contributions

R.Z. conceptualized; K.N., A.K., T.V., and D.L. developed investigational methods; K.N., A.K., and T.V. conducted the formal analysis, K.N., A.K. and R.Z. wrote the original draft, E.B. and R.Z. supervised the work.All authors have read and agreed to the published version of the manuscript.All authors reviewed the manuscript.

Funding
This research was supported by the Semmelweis Science and Innovation Fund (STIA-KF-2022.This research was funded by the NVKP_16-1-2016-0004 grant of the Hungarian National Research, Development and Innovation Office (NKFIH), VEKOP-2.3.2-162016-00002, VEKOP-2.3.3-15-2017-00016, the Therapeutic Thematic Programme TKP2021-EGA-23. This study was also supported by the grants RRF-2.3.121-2022-00003 (National Cardiovascular Laboratory Program), 2019 – 2.1.7-ERA-NET-2021-00015 and János Bolyai Research Scholarship of the Hungarian Academy of Sciences. The project has received funding from the EU's Horizon 2020 Research and Innovation Programme under grant agreement No. 739593.

Declarations

Competing interests
The authors declare no competing interests.

Additional information
Supplementary Information The online version contains supplementary material available at https://doi.org/10.1038/s41598-024-79277-3.

Correspondence and requests for materials should be addressed to R.Z.

Reprints and permissions information is available at www.nature.com/reprints.

Publisher's note Springer Nature remains neutral with regard to jurisdictional claims in published maps and institutional affiliations.